

Systematic Studies on 3 d- and 4 f-Metal Containing Polyoxometalates Suitable for Organic Derivatization**

Beñat Artetxe*[a]

Awarding Institute: Universidad del País Vasco UPV/EHU (Spain)

Date Awarded: June 23, 2014

Supervisors: Dr. Santiago Reinoso and Prof. Dr. Juan M. Gutiérrez-Zorrilla, Universidad del País Vasco UPV/EHU, Bilbao (Spain)

Polyoxometalates (POMs) form a well-known class of anionic oxo-bridged early transition metal clusters that show remarkable structural and compositional diversity and potential applications in fields like catalysis, biomedicine, or materials science. Heteropolyoxotungstates represent the most studied family among the different classes of POMs, and they contain not only metal and oxygen, but also additional elements known as heteroatoms. Removal of $(M=O)^{n+}$ groups from the inorganic POM skeleton results in the so-called lacunary species that can act as multidentate O-donor ligands toward different types of electrophiles. Derivatization of POMs with additional organic functions represents one of the most relevant topics in the field at present. The resulting hybrids have been identified as a key factor for the clusters to be suitably incorporated into polymeric materials or carbon nanotubes, firmly anchored on diverse surfaces (e.g., oxides, metals, graphite), or even to interact with metallic nanoparticles. The use of tailored POM hybrids for constructing such composites might pave the way for new multifunctional devices like immobilized catalysts or photoactive systems for energy conversion and storage. However, this usually requires elaborate organic functions that can be achieved only via multi-step synthetic work on so-called preformed hybrid POM platforms.


Different approaches have been applied to prepare solution-stable hybrid POMs on a precursor scale: 1) Combination of lacunary Keggin or Wells–Dawson polyoxotungstates with *p*-block organoderivatives such as organosilyl, -germyl, -phosphoryl, or -stannyl moieties; 2) Replacement of shell O atoms with O- or N-donor ligands, as exemplified by the series of tris(alkoxo)-capped Anderson–Evans anions or the different organoimido and diazenido derivatives of Lindqvist-type molybdates; 3) Grafting of transition metal complexes on POM surfaces; 4) Coordination of organic molecules to suitable d- or f-metal-substituted POMs with exposed metal centers showing labile terminal ligands (e.g. aqua, acetato).

The aim of this dissertation is based on the last synthetic approach and consists in exploring the viability of classical coordination chemistry for the organic functionalization of well-known clusters with accessible metal centers, as well as in preparing new POMs with exposed 3 d or 4 f-metal centers potentially suitable for this type of organic derivatization. Therefore, this work has been divided into two well distinguished parts: in the first one, a systematic study on the organic functionalization of transition-metal-disubstituted Krebs-type POMs with different N,O-chelating and N,O-bis(bidentate) bridging

[a] Dr. B. Artetxe

Departamento de Química Inorgánica, Facultad de Ciencia y Tecnología
Universidad del País Vasco UPV/EHU, P.O. Box 644, 48080 Bilbao (Spain)
E-mail: benat.artetxe@ehu.es

[**] The full thesis is available from the Universidad del País Vasco UPV/EHU official repository on the WWW under <http://hdl.handle.net/10810/14962>. Please note that Wiley-VCH is not responsible for the content or functionality of the full thesis. Any queries should be directed to the corresponding author of the Thesis Summary.

 The ORCID from the author of this article is available on the WWW under <http://dx.doi.org/10.1002/open.201500221>.

 © 2015 The Authors. Published by Wiley-VCH Verlag GmbH & Co. KGaA.

This is an open access article under the terms of the Creative Commons Attribution-NonCommercial-NoDerivs License, which permits use and distribution in any medium, provided the original work is properly cited, the use is non-commercial and no modifications or adaptations are made.

organic ligands is reported, whereas the second part includes the synthesis and full characterization of some new 4 f-metal containing clusters or 3 d/4 f heterometallic species.

Functionalization of Krebs-type polyoxometalates with N,O-chelating ligands

Transition-metal-disubstituted Krebs-type tungstoantimonates(III) with general formula $[\{M(H_2O)_3\}_2\{WO_2\}_2(Sb^III W_9O_{33})_2]^{10-}$ (where $M^{II} = Mn, Co, Ni, Zn$) could be ideal candidates to perform straightforward derivatizations through the replacement of labile aqua ligands with organic molecules because 1) they show six accessible water molecules, 2) they are stable in solution over a wide pH range and can be prepared in large amounts, and 3) their structure allows multiple compositional variations to be carried out. Thus, a systematic investigation on the reactivity of 3 d-metal-substituted Krebs-type POMs toward N,O-chelating or bridging ligands has been undertaken to determine whether this family of POMs is suitable for being functionalized via classical coordination chemistry under mild conditions and to find out which ligands are the most appropriate for this purpose.

In a first step, planar carboxylate derivatives of five- and six-membered *N*-donor heterocycles were selected, and more specifically, diazole-, pyridyl-, and diazinecarboxylates with chelating ability. Reactions between POM clusters (preformed or generated in situ starting either from the corresponding Keggin-type trilacunary species or from a mixture of tungstate with heteroatom and 3 d-metal sources) and 1 H-imidazole-4-carboxylate (imc), 1 H-pyrazole-3-carboxylate (pzc), picolinate (pic), pyridazine-3-carboxylate (pydc), pyrimidin-4-carboxylate (pymc) or pyrazine-2-carboxylate (pyzc) ligands were performed in buffered sodium acetate medium under mild bench conditions. To determine the success of these functionalization attempts prior to X-ray diffraction (XRD) studies, infrared (IR) spectroscopy was used to characterize any solid product (crystalline or not) obtained from the above reactions. This technique proved to be excellent for this aim because 1) bands associated to inorganic clusters and organic ligands are located in different regions of the spectra and 2) significant variations take place in the POM domain upon functionalization.

Derivatization of Krebs-type POMs showed to be extremely dependent on the specific nature of the ligand. For example, the imc anion has been identified as a "universal" ligand because it undergoes coordination regardless of the 3 d metal or the reaction conditions, whereas the closely related pzc either showed selectivity toward the functionalization of the Ni precursor or promoted partial decomposition of the Co analogue to give the complex $[Co(pzc)_2(H_2O)_2]$ (**Co-pzc**). Selective behavior toward the Co and Zn precursors has also been observed for pyzc, but in contrast, the use of the other diazinecarboxylates (pydc and pymc) resulted in the corresponding $[M^II L_2(H_2O)_2]$ complexes (**Co-pydc**, **Ni-pydc**, and **Co-pymc**), while picolinate was found to be inert under all of the conditions tested. In addition, the imc ligand was also used to gain further insight into the influence of the heteroatom on the reactivity of the Krebs-type anions by replacing Sb^{III} with Te^{IV} . Functionalization showed to be selective toward the Mn and Co derivatives. These systematic studies have resulted in the preparation of nine pure crystalline phases of general formula $[\{ML(H_2O)_2\}_2(WO_2)_2(B-\beta-XW_9O_{33})_2]^{7-}$ that have been characterized by means of elemental analyses, thermogravimetric analyses (TGA) and single-crystal XRD. These compounds can be classified as follows (Figure 1): **1-SbM**, where $L = imc$, $X = Sb$, $n = 12$, and $M = Mn, Co, Ni, Zn$; **1-TeM**, where $L = imc$, $X = Te$, $n = 10$, and $M = Mn, Co$; **2-SbNi**, where $L = pzc$, $X = Sb$, $n = 12$, and $M = Ni$; and **3-SbM**, where $L = pyzc$, $X = Sb$, $n = 12$, and $M = Co, Zn$. It is worth mentioning that the 3 d-metal-disubstituted Krebs-type skeleton of the tungstotellurate analogues is completely unprecedented in POM chemistry. According to XRD studies, the organic ligands replace in all cases the same two water molecules of the parent Krebs-type POM in such a way that they adopt a similar orientation with respect to the POM skeleton that allows the formation of intramolecular C–H...O or N–H...O type hydrogen bonds depending on the nature of the ligand. Furthermore, the hybrid species reported herein are stable in aqueous solution according to 1H NMR studies performed on the diamagnetic Zn derivatives.

The study was later extended to other molecules with bridging ability. Ligands like 4,4'-bipyridine (4,4'-bpy) were tested, but the study mainly focused on the planar *N,O*-bis(bidentate) linkers pyrazine-2,3- and -2,5-dicarboxylate (2,3- and 2,5-pydc). Derivatization of Krebs-type POMs with bridging ligands applying the same synthetic conditions described above proved to be again fully dependent on the specific nature of the latter. For example, the *N,N*-bis(monodentate) 4,4'-bpy showed to be inert toward Krebs-type POMs, and the reactions led to the series of compounds $Na_{10}[\{M(H_2O)_3\}_2(WO_2)_2(SbW_9O_{33})_2] \cdot 2(4,4'-bpy) \cdot 32H_2O$ (**4-M**, $M = Mn, Co, Ni, Zn$) where 4,4'-bpy molecules occupy interstitial positions among pristine Krebs-type anions according to XRD studies. Regarding

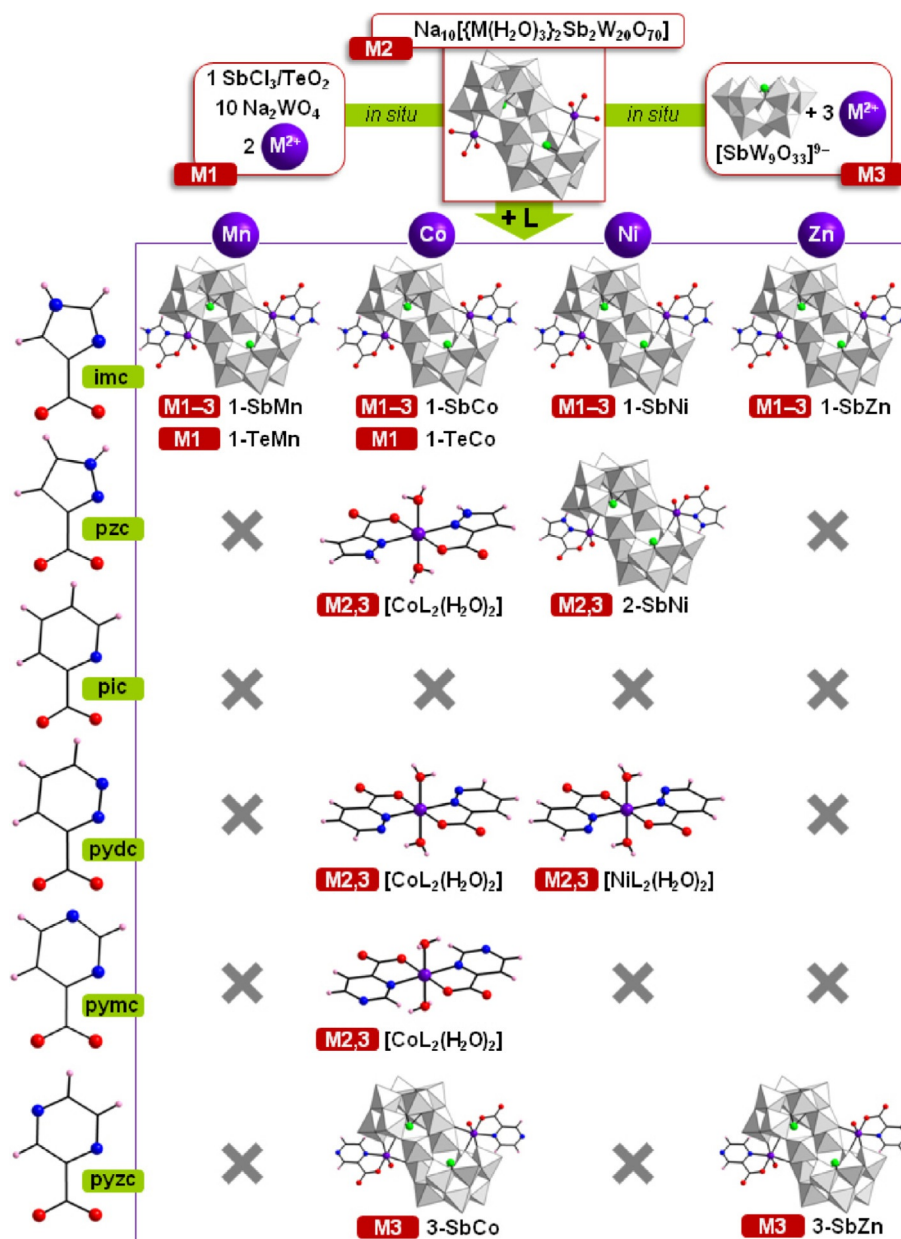


Figure 1. Synthetic approaches for compounds 1-SbM (M=Mn, Co, Ni, Zn), 1-TeM (M=Mn, Co), 2-SbNi, and 3-SbM (M=Co, Zn). Color code: WO₆, gray octahedra; Sb or Te, green; 3 d metal, violet; O, red; N, blue; H, pink.

N,O-bis(bidentate) linkers, it is worth mentioning that while 2,5-pyzdc is inert, 2,3-pyzdc shows selective reactivity toward the nickel containing cluster. In this case, the attack of the ligand promotes a rearrangement of the tungsten-oxygen skeleton to result in the dimeric $[\mu\{-2,3\text{-pyzdc}\}_2\{\text{Ni}_2(\text{H}_2\text{O})\text{Sb}_2\text{W}_{20}\text{O}_{70}\}_2]^{24-}$ (5-Ni) hybrid polyanion. This species is formed by two unprecedented 20-tungsto-2-antimonate(III) clusters linked by two *N,O*-bis(bidentate) bridging ligands. Alternatively, each half of 5-Ni can also be seen as a defective Ni-containing POM with one Na-blocked vacant site (Figure 2), and hence, it could be a good candidate for incorporating additional electrophiles. The dimeric assembly undergoes full dissociation in water that can be partially hindered upon addition of acetone as identified by electrospray ionization-mass spectrometry (ESI-MS). Its magnetic properties are dominated by the zero-field splitting of Ni^{II} centers.

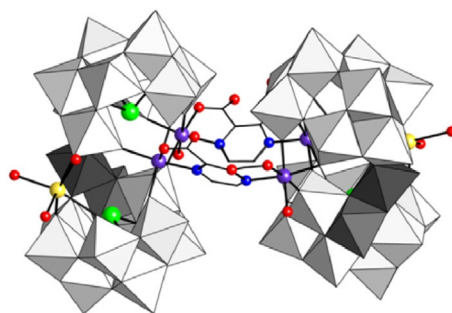


Figure 2. Structure of 5-Ni with the Na-blocked positions shown in yellow (dark gray for the $\{W_2O_{10}\}$ moiety).

Structural diversity in lanthanide-containing tungstogermanate assemblies

One-pot reaction of lanthanide(III) ions, GeO_2 and Na_2WO_4 in sodium acetate buffer results in a library of $[Ln_2(GeW_{10}O_{38})]^{6-}$ clusters which consist of dilacunar Keggin fragments stabilized by the coordination of 4 f-metal atoms to the vacant sites and show the ability to undergo cation-directed association processes. The use of early lanthanides (La to Sm) together with Ni^{2+} aqua complexes as crystallizing agent leads to hexameric crown-shaped $[Na \subset Ln_{12}Ge_6W_{60}O_{228}(H_2O)_{24}]^{35-}$ (**6-Ln**, Ln = Pr, Nd) architectures formed by alternating $\beta(1,5)/\beta(1,8)$ enantiomeric subunits in the exclusive presence of Na^+ , whereas the addition of K^+ results in a similar kind of assembly $[K \subset Sm_{12}Ge_6W_{60}O_{228}(H_2O)_{22}]^{35-}$ (**7-Sm**) for Sm and giant dodecameric structures $[K \subset Ce_7Ln_{24}Ge_{12}W_{120}O_{444}(OH)_{12}(H_2O)_{56}]^{52-}$ (**8-Ln**) for Ce, Pr and Nd. The latter species exhibit a central hexameric core virtually identical to **7-Sm**, to which six external $\gamma(3,4)$ -subunits are linked. The dimeric $[Ln_4(H_2O)_6(\beta-GeW_{10}O_{38})_2]^{12-}$ (**9-Ln**, Ln = Gd to Lu) entities were obtained by employing mid-to-late lanthanides (Gd to Lu) under the same synthetic conditions but in the absence of any crystallizing agent. When Cs^+ was added, two dimeric species further assemble into the $[[Ln_4(H_2O)_5(GeW_{10}O_{38})_2]_2]^{24-}$ tetramers (**10-Ln**, Ln = Ho to Lu). Two types of such tetrameric anions coexist in the solid state: one shows a full $\beta\beta$ -architecture, whereas the other one is a mixed $\alpha\beta$ -assembly in which each β -subunit is linked to its corresponding α derivative. All the families (Figure 3) have been characterized by elemental analyses, TGA, IR, and XRD. Luminescent properties of **7-Sm**, **9-Tb**, and **9-Dy** have been studied and correlated with the crystal structure, in such a way that the lanthanide ions showing edge-sharing linkages with adjacent $\{WO_6\}$ octahedra have been identified as the only efficient emitting centers. In addition, the magnetic properties in the **9-Ln** series have also been analyzed.

Regarding the solution behavior, combined ESI-MS and ^{183}W NMR spectroscopy experiments indicate that the **10-Ln** tetramers fully fragment into **9-Ln**-like dimers upon dissolution in water, which in turn undergo partial dissociation into their corresponding monomers and slow dimer/monomer equilibration. This is most likely followed by a β -to- α isomerization of monomeric clusters with consequent re-assembly into dimeric anions, as indicated by the isolation of three additional crystalline phases of $\alpha\alpha$ -**9-Ln** derivatives. The solution behavior of compounds **8-Ln** is even more complex. The dodecameric anions dissociate upon dissolution in water into their hexameric cores and monomeric entities, as identified by ESI-MS studies. The former self-assemble into spherical, hollow, and single-layered vesicle-like *blackberry*-type structures of about 75 nm radii, as monitored by dynamic (DLS) and static (SLS) light scattering techniques and confirmed by transmission electron microscopy (TEM). Analogous studies performed for **8-Nd** in water/acetone mixtures show that the dodecamers remain stable and are able to form in turn their own type of *blackberries* with sizes increasing from ~20 to 50 nm with the acetone concentration. This control over both the composition and size of the vesicle-like assemblies is achieved for the first time by modifying the architecture of the species undergoing supramolecular association through variations in the solvent polarity (Figure 4).

Heterometallic 3d–4f polyoxometalates derived from the Krebs-type framework

The combination of preformed or in-situ-generated $[[M(H_2O)_3]_2(WO_2)_2(B-\beta-SbW_9O_{33})_2]^{10-}$ ($M=Co, Ni, Zn$) Krebs-type anions with early lanthanides (La to Gd) in sodium acetate buffer promotes the rearrangement of the parent anion to lead to the formation of the heterometallic species $[Sb_7W_{36}O_{133}Ln_3M_2(OAc)(H_2O)_8]^{17-}$ (**11-LnM**, Ln = La to Gd, $M=Co$; Ln = Ce, $M=Ni, Zn$; Figure 5). Compounds **11-LnM** have been characterized by means of elemental analyses, TGA, and IR. According to

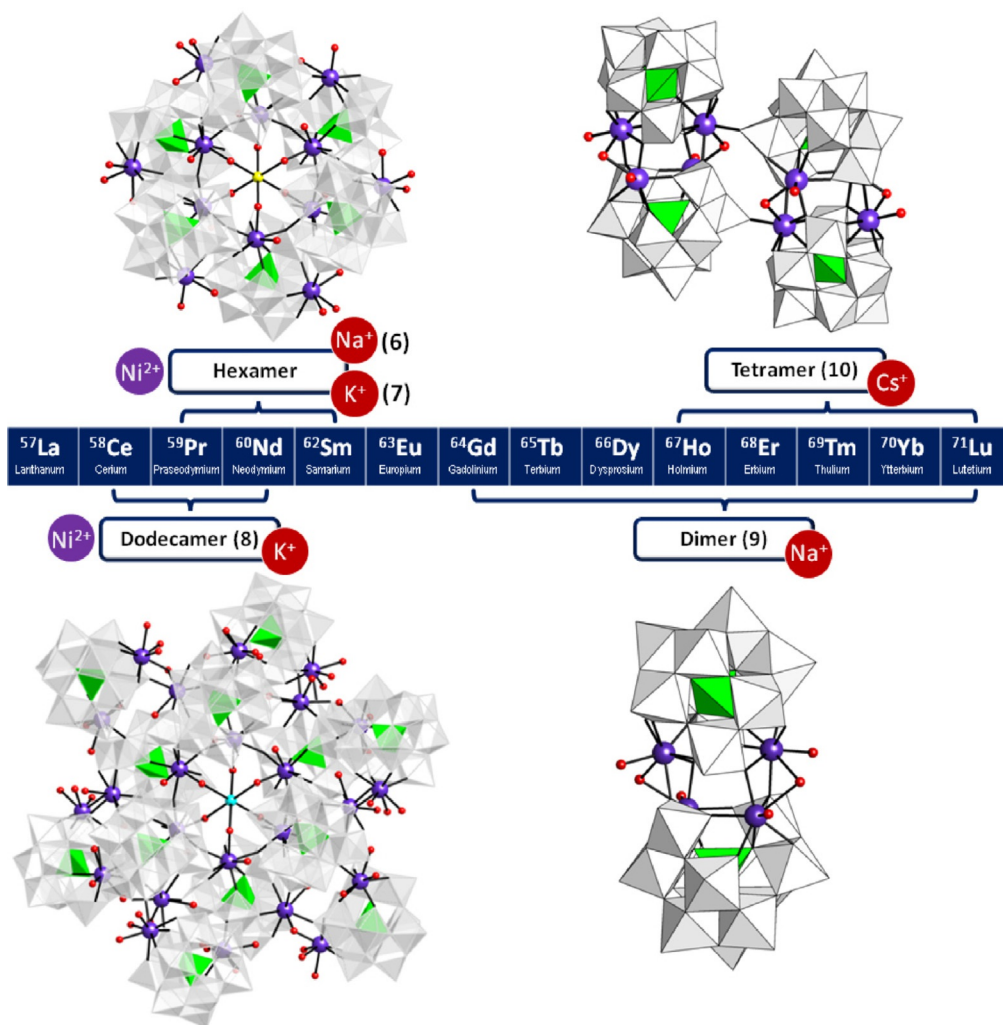


Figure 3. Molecular structures of compounds **6-Ln** (Ln=Pr, Nd), **7-Sm**, **8-Ln** (Ln=Ce to Nd), **9-Ln** (Ln=Gd to Lu), and **10-Ln** (Ln=Ho to Lu). Color code: WO_6 , gray octahedra; GeO_4 , green tetrahedra; 4f metal, violet; O, red; Na/K, yellow; K, blue.

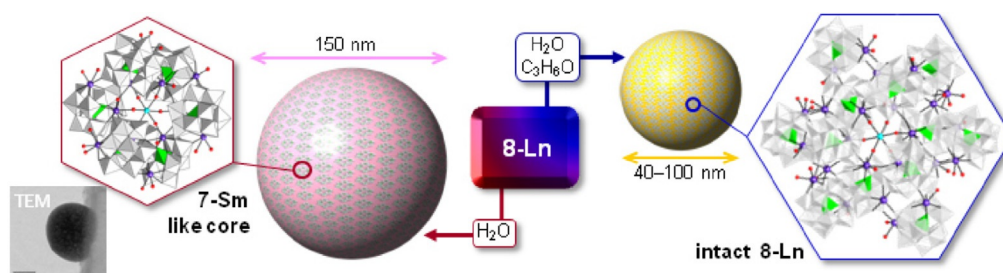


Figure 4. Schematic representation of the solvent-dependent *blackberry* formation for compounds **8-Ln**.

XRD studies, the molecular structure of the **11-LnM** anions consist of a tetrameric assembly of three Keggin-type $\{\text{B-}\alpha\text{-SbW}_9\text{O}_{33}\}$ trilacunary subunits and one $\{\text{MW}_6\text{O}_{24}\}$ Anderson–Evans-type fragment. The trilacunary subunits are linked to each other by two nine-coordinated 4f-metal atoms and one $\{\text{LnM}(\mu\text{-OAc})\}$ dimer, whereas the capping $\{\text{MW}_6\text{O}_{24}\}$ fragment is connected to the former via three additional $\{\text{WO}_2\}$ groups. The tetrameric POM framework described above encapsulates the unusual $\{\text{Sb}_4\text{O}_4\}$ cluster, which confers chirality on the **11-LnM** anions by arranging in left- or right-handed orientations due to a pivoting motion on one of its Sb centers. Compounds **11-LnM** represent the first example where an Anderson–Evans anion acts as a fragment of larger POM skeletons by establishing W–O–W

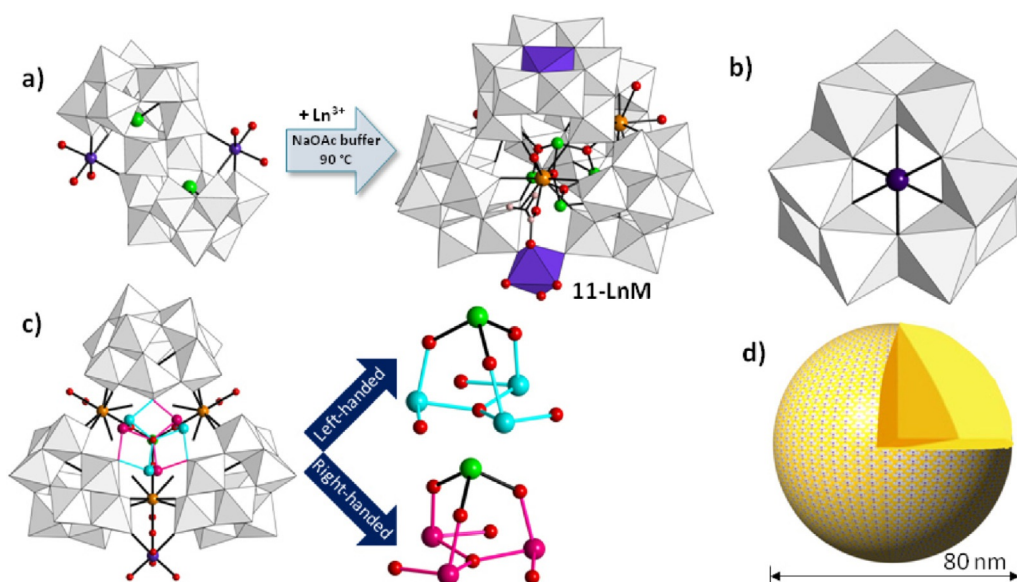


Figure 5. a) Formation of **11-LnM**. b) Structure of the $\{MW_9O_{33}\}$ capping unit. c) View of **11-LnM** highlighting the enantiomerically related left- (blue) and right-handed (pink) orientations of the $\{Sb_4O_7\}$ cluster (capping unit omitted for clarity). d) Supramolecular *blackberry*-type assembly formed in diluted aqueous solutions. Color code: M, purple; Ln, orange.

linkages, and the $\{MW_9O_{33}\}$ subunit formed upon its condensation with the three $\{WO_2\}$ groups constitutes a novel building block in POM chemistry. The cluster is stable in aqueous solution, as confirmed by ESI-MS studies carried out for the **11-CeCo** derivative. This anion undergoes a self-assembly process in diluted solutions to form *blackberry*-type structures, as monitored by DLS and SLS experiments and confirmed by TEM images. The electron paramagnetic resonance spectra of **11-CeCo** and **11-GdCo** are consistent with the 1D-arrangement of hydrogen-bonded clusters found in the crystal structure.

Keywords: polyoxometalates · self-assembly · solution studies · supramolecular chemistry · X-ray diffraction

Publications arising from this work:

- B. Artetxe, L. San Felices, A. Pache, S. Reinoso, J. M. Gutiérrez-Zorrilla, *Acta Crystallogr. Sect. E* **2013**, *69*, m94–m95.
- B. Artetxe, S. Reinoso, L. San Felices, J. Martín-Caballero, J. M. Gutiérrez-Zorrilla, *Acta Crystallogr. Sect. E* **2013**, *69*, m420–m421.
- B. Artetxe, S. Reinoso, L. San Felices, L. Lezama, J. M. Gutiérrez-Zorrilla, J. A. García, J. R. Galán-Mascarós, A. Haider, U. Kortz, C. Vicent, *Chem. Eur. J.* **2014**, *20*, 12144–12156.
- B. Artetxe, S. Reinoso, L. San Felices, P. Vitoria, A. Pache, J. Martín-Caballero, J. M. Gutiérrez-Zorrilla, *Inorg. Chem.* **2015**, *54*, 241–252; associated Cover Art for *Vol. 54, Issue 1*, 2015.
- B. Artetxe, S. Reinoso, L. San Felices, L. Lezama, A. Pache, C. Vicent, J. M. Gutiérrez-Zorrilla, *Inorg. Chem.* **2015**, *54*, 409–411.
- B. Artetxe, S. Reinoso, L. San Felices, J. M. Gutiérrez-Zorrilla, J. A. García, F. Haso, T. Liu, C. Vicent, *Chem. Eur. J.* **2015**, *21*, 7736–7745; associated *Frontispiece*-type cover.
- B. Artetxe, S. Reinoso, L. San Felices, L. Lezama, J. M. Gutiérrez-Zorrilla, F. Haso, T. Liu, C. Vicent, *Chem. Eur. J.* **2015**, DOI: 10.1002/chem.201504768.

Received: December 15, 2015
Published online on January 12, 2016